Eur. Phys. J. D **15**, 229–235 (2001)

THE EUROPEAN PHYSICAL JOURNAL D

EDP Sciences

Numerical studies on velocity, temperature history and heat transfer to the particles injected into the argon plasma

R. Ramasamy and V. Selvarajan[a]

Department of Physics, Bharathiar University, Coimbatore, 641 046 Tamil Nadu, India

Received 4 May 2000 and Received in final form 15 March 2001

Abstract. A new approach to study the particle velocity in a thermal plasma in relation to input parameters (power, gas flow rate, injection velocity of the particle and particle size) and nozzle dimensions (nozzle length and diameter) has been made. Injected particle's temperature and thermal history were calculated for particles of three different materials (alumina, tungsten and graphite) in argon plasma. Allowable powder feed rate was calculated for the particles. Heat transfer per particle injected in to the plasma is reported. Liquid fraction of the particle after it reached the melting point is also reported. Particle velocity is found to increase with increase in power, gas flow rate and injection velocity and decrease with increase in particle size, nozzle length and nozzle diameter. Thermal histories of the particles in relation to the plasma temperature and particle diameter are presented. Particle's residence time is found to increase with increase in diameter of the particle. Allowable powder feed rate for complete melting of the particle is higher at higher percentage utilisation of the plasma power. Powder feed rate is seen to decrease with increase in particle size and it is higher for tungsten and lower for graphite particle. Heat transfer rate from plasma to particle is seen to decrease with increase in time and the same is higher for plasmas of higher temperature and smaller sized particle.

PACS. 52.75.Hn Plasma torches – 52.77.-j Plasma applications – 52.80.Mg Arcs; sparks; lightning; atmospheric electricity

1 Introduction

The use of plasmas for various applications has gained considerable importance in recent years [1]. Examples are large-scale diamond deposition [2], surface modification, chemical conversion, synthesis of ultra fine powder and non-oxide ceramic powders [3] and effluent gas treatment. Such plasmas are characterized by very large density and a high degree of activation.

The understanding of the particle velocity, thermal histories and plasma-particle heat transfer are the important areas of study in thermal plasma processing. A good knowledge of these phenomena is necessary to improve the quality of the process [4].

Several researchers have carried out fundamental studies in plasma-particle heat and momentum transfers [5–16], trajectories and temperature history [5–11, 17–20] of the particle in flight. Except Das *et al.* [18] and Ramachandran *et al.* [17] the assumptions made in most of these studies are not consistent with prevailing conditions in plasma spraying. Das *et al.* [18] concluded that assumptions of a single average temperature in the calculation of particle velocity and temperature histories are not correct.

Park *et al.* [19] studied the plasma-particle interaction using LTE (local thermodynamic equilibrium) model for rf plasma jet. Bauchire *et al.* [20] studied the interaction between argon plasma at atmospheric pressure and metallic powders in a DC plasma torch using PSI cell model [21].

It appears that no investigator has reported the effect of all the parameters (input power, gas flow rate, nozzle diameter, nozzle length, particle size and injection velocity) simultaneously on particle velocity.

In plasma spraying, input power (E), gas flow rate (G), nozzle length (L), nozzle diameter (D), plasma temperature (T_∞), particle size (d_p) and its injection velocity ($V_{\mathrm{p}0}$) are important parameters in deciding the quality of the coatings. In the present paper the results of a study of particle velocity for different E, G, L, D, T_∞, d_p and $V_{\mathrm{p}0}$, temperature histories of the alumina, tungsten and graphite particles in an argon plasma for different T_∞ and d_p are reported. Liquid fraction of the particle after reaching the melting point, rate of heat transfer to each particle as a function of time during its flight in the torch and allowable powder feed rate are also reported.

[a] e-mail: vselvrjn@bharathi.ernet.in
or e-mail: physics@as250bharathi.ernet.in

2 Basic equations and methodology

For the present study, heating of a single particle is considered. The integral mean values of the plasma properties ($\overline{\mu}$: viscosity, $\overline{k}$: thermal conductivity and $\overline{\nu}$: kinematic viscosity) are used due to the steep temperature gradient between the particle and plasma. Thermophysical constants of the argon plasma and alumina particle used in the calculations were taken from the available literature [22,23].

The equations governing the momentum and heat transfer between the particles and the plasma can be written as follows:

$$(\mathrm{d}V_\mathrm{p}/\mathrm{d}t) = (3/4)\, C_\mathrm{Dc}(V_\mathrm{p} - V_\mathrm{g})|V_\mathrm{p} - V_\mathrm{g}|(\rho_\mathrm{f}/\rho_\mathrm{p} d_\mathrm{p}) \quad (1)$$

where C_Dc is the drag coefficient given by the following correlations as a function of the Reynolds number ($Re = \rho_\mathrm{f}|V_\mathrm{p} - V_\mathrm{g}|d_\mathrm{p}/\mu_\mathrm{f}$), where ρ_f and μ_f are the values of densities and viscosities of the plasma gas evaluated at the film temperature and d_p is the diameter of the particle

$$\begin{array}{lll} C_\mathrm{Df} = 24/Re & \text{for} & Re < 0.2, \\ C_\mathrm{Df} = (24/Re)(1 + 0.187Re) & \text{for} & 0.2 \le Re < 2, \\ C_\mathrm{Df} = (24/Re)(1 + 0.110\, Re^{0.81}) & \text{for} & 2.0 < Re \le 21.0. \end{array}$$

The following correction factor is included for the steep temperature gradient in the plasma. This correction factor is considered as a valid approximation in a plasma [14]

$$C_\mathrm{Dc} = C_\mathrm{Df}(\rho_\infty \mu_\infty/\rho_\mathrm{w}\mu_\mathrm{w})^{-0.45} \quad (2)$$

f, ∞ and w denote properties corresponding to the film ($T_\mathrm{f} = (T_\infty + T_\mathrm{w})/2$), plasma and wall temperatures.

So far [5–15,17–19] the average velocity of the plasma jet V_g and plasma temperatures were taken as arbitrary values. In our study the calculations are made on the V_g in relation to E, G, L and D using the enthalpy values calculated from the energy balance equations [24,25] as follows.

The energy balance in the plasma spray torch is the energy gained by the gas which is the difference between the electrical input and the total coolant and external losses. This may be stated as follows:

$$[\text{Energy In}] - [\text{Energy Loss}] = [\text{Energy in plasma}] \quad (3)$$

where

$$(Q_\mathrm{T} - Q_\mathrm{L}) = Q_\mathrm{G}$$

$$Q_\mathrm{T} = VI = E$$

$$Q_\mathrm{L} = W_\mathrm{c} C_\mathrm{pc}(\Delta T_\mathrm{f} - \Delta T_0)$$

and

$$Q_\mathrm{G} = W_\mathrm{g} H_\mathrm{g} - W_\mathrm{g} H_\mathrm{0g}$$

The electrothermal efficiency is given by the equation:

$$\eta = \frac{Q_\mathrm{G}}{VI} \times 100 \quad (4)$$

where H_g is the enthalpy of the plasma jet (J/kg) and W_g is the flow rate of the plasma- forming gas (kg/s)

$$H_\mathrm{g} = \frac{W_\mathrm{g} H_\mathrm{0g} + VI - W_\mathrm{c} C_\mathrm{pc}(\Delta T_\mathrm{f} - \Delta T_0)}{W_\mathrm{g}} \quad (5)$$

where H_0g: enthalpy of incoming gas (J/kg), ΔT_f: temperature rise in coolant with arc operating (K), ΔT_0: temperature rise in the coolant without arc operating (K), W_c: mass flow rate of the coolant (kg/s) and C_pc: specific heat capacity of the coolant (J/kg K).

The empirical equation to calculate the yield of a cascade torch with gas injection is given by [24]:

$$\frac{1-\eta}{\eta} = 5.85 \times 10^{-5}\, [I^2/GD]^{0.265} \times\ [PD]^{0.3}\ [G/D]^{-0.265}\ [L/D]^{0.5} \quad (6)$$

where P: pressure (N/m^2) and G: gas flow rate (l/min).

Using equations (4, 6) the rise in cooling water temperature was calculated for different values of current, flow rates and nozzle dimensions from which the enthalpy of the plasma jet were determined. The enthalpy value was used to calculate the velocity of the plasma jet in relation to the mass flow rate of the gas (W_g) and average density of the plasma gas (ρ) is given by [25]:

$$V_\mathrm{g} = \frac{W_\mathrm{g}}{(\pi/4)D^2\rho}\,. \quad (7)$$

The particle temperature is calculated by solving the following equation:

$$mC_\mathrm{p}(\mathrm{d}T_\mathrm{p}/\mathrm{d}t) = a_\mathrm{p} h(T_\infty - T_\mathrm{p}) - a_\mathrm{p}\varepsilon\sigma(T_\mathrm{p} - T_\mathrm{a}) \quad (8)$$

where m: mass of the particle (kg), C_p: specific heat capacity of the particle (J/kg K), a_p: area of the particle (m^2), ε-emissivity of the particle and σ-Stefan constant.

The heat transfer co-efficient, h (W/m^2 K) ($h = Nu/d_\mathrm{p}\overline{k}$, $\overline{k}$-integrated mean thermal conductivity of the plasma) was calculated using the Ranz and Marshall [9] correction. A kinematic viscosity ratio to the power 0.15 was also used as a correction factor due to the presence of steep temperature gradients as given by equation:

$$Nu = (2.0 + 0.151Re^{0.5})(\nu_\mathrm{av}/\nu_\infty)^{0.15}. \quad (9)$$

Solving equation (1) we get the particle velocity and by solving equation (8) we get the temperature histories of the particle.

As the particle reached its melting point its temperature was assumed to remain constant. The liquid fraction, x, of the particle was then calculated using the following equation:

$$\mathrm{d}x/\mathrm{d}t = ha_\mathrm{p}(T_\infty - T_\mathrm{p}) - a_\mathrm{p}\sigma\varepsilon(T_\infty - T_\mathrm{a})/(m\lambda_m). \quad (10)$$

Once the particle was completely molten, $x = 1$, its temperature could rise again till its boiling temperature was reached.

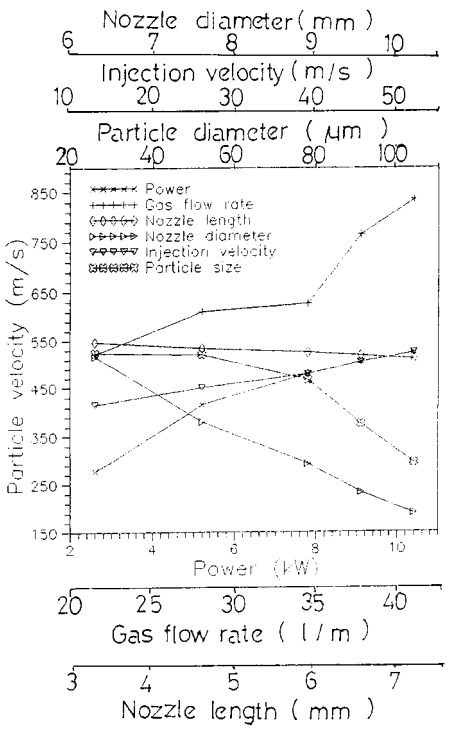

Fig. 1. Particle velocity as a function E, G, L, D, d_p and $V_{\mathrm{p}0}$.

The allowable powder feed rate, A_p was determined using the following equation:

$$A_\mathrm{p} = (\alpha Q_\mathrm{G}/Q)m \tag{11}$$

where α is the fraction of the power in the plasma, Q_G, that could be used to heat the particles and m, the mass of each particle and Q is the total heat load transferred to the particle. The values of α are calculated from the electrothermal efficiency of the plasma torch using the energy balance equations (4–6)

$$Q = \int_0^{t_\mathrm{r}} h a_\mathrm{p}(T_\infty - T_\mathrm{p})\mathrm{d}t. \tag{12}$$

Heat transfer rate per particle at time t is $h_\mathrm{r} = h a_\mathrm{p}(T_\infty - T_p)$. Equations (1, 8, 10, 12) were solved using numerical methods.

3 Results and discussion

3.1 Particle velocity

The particle velocity (V_p) at the 10th ms after the injection of the particle into the plasma flame as a function of input power (E), gas flow rate (G), nozzle dimensions (nozzle length L and diameter D), injection velocity($V_{\mathrm{p}0}$) and particle diameter (d_p) are shown in Figure 1. V_p is seen to increase with increase in power. An increase in power will increase the energy of the arc plasma, which in turn will increase of the velocity of the plasma jet.

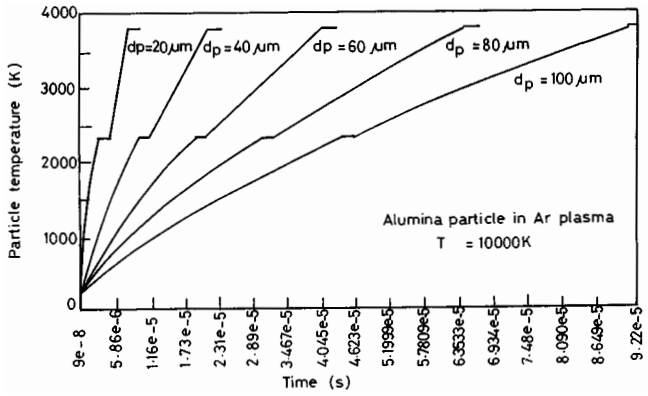

Fig. 2. Temperature of the alumina particle as a function of time for selected values of particle diameter.

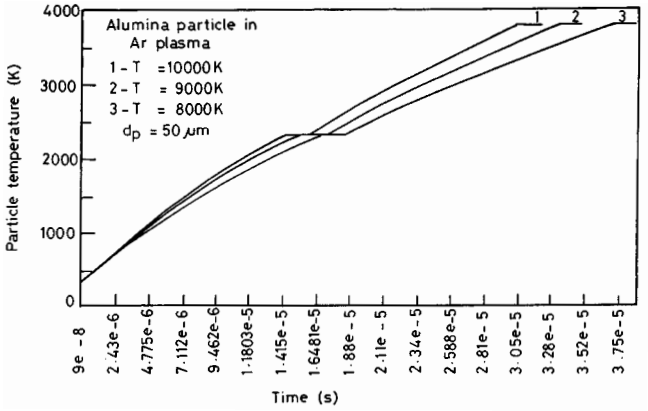

Fig. 3. Temperature of the alumina particle as a function of time for selected values of plasma temperature.

Increase in flow rate of the plasmagen gas will directly increase the velocity of the plasma jet which in turn will increase V_p.

V_p is found to decrease with increase in nozzle length and nozzle diameter. This is due to the fact that the plasma jet velocity will decrease with increase in nozzle diameter and nozzle length [24,25]. The effect of variation of nozzle length on V_p is not very significant.

Further V_p increases with increase in injection velocity and decreases with increase in particle size.

3.2 Temperature history

The temperature history of the alumina particle from its injection up to its evaporation is illustrated in Figures 2 and 3, for selected values of particle size and plasma temperature respectively. The particle temperature increases with increase in time. The smaller the size of the particle more efficient is the heat transfer from plasma to the particle. Melting point can be identified on the characteristics which is the same (Fig. 3) for all the cases indicating the accuracy of calculations. At higher temperatures (Fig. 3) alumina particles gain temperature at a faster rate, even though the increase in rate is not very significant.

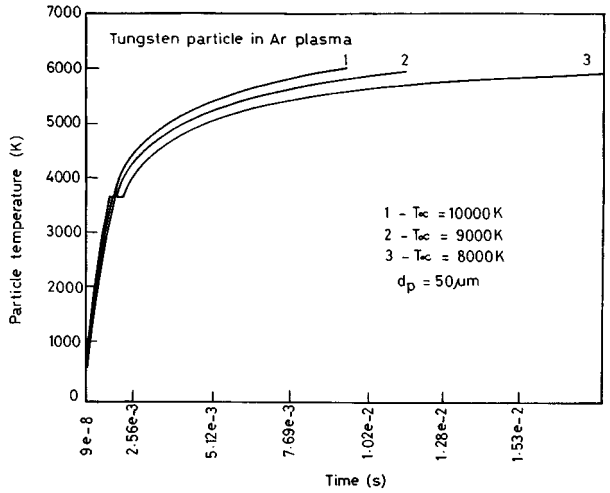

Fig. 4. Temperature history of the tungsten particle during its trajectory at selected values of plasma temperatures.

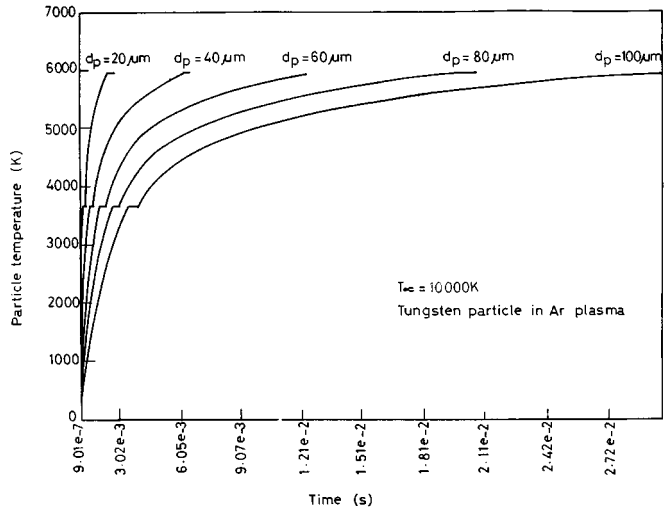

Fig. 5. Temperature history of the tungsten particle during its trajectory at selected values of particle diameter.

For example for plasma at 10 000 K the melting of particles occurs after 4.90 ms after injection and the same for plasma at 8 000 K is 5.71 ms. For tungsten particle, (Figs. 4 and 5) both for different sizes of particles and for different plasma temperatures the particle temperature increases with increase in time. After melting the temperature tends to saturate against time.

For graphite particle (Figs. 6 and 7) the temperature increase is gradual with increase in log time. For a given size of the particle and plasma temperature, at time $t = 3.0$ ms the rate of increase in temperature is 0.061, 1.545 and 0.118 K/s for alumina, tungsten and graphite respectively. The heat capacities of the materials are 1.882, 0.206 and 1.006 J s/kg K respectively. The temperature histories are in agreement with the earlier results [5–11,16–19].

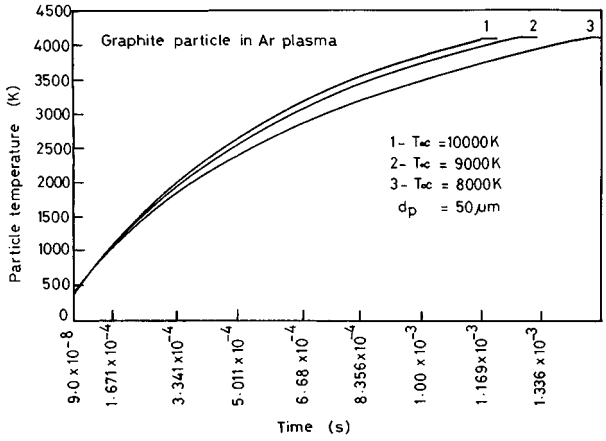

Fig. 6. Temperature history of the graphite particle during its trajectory for selected plasma temperatures.

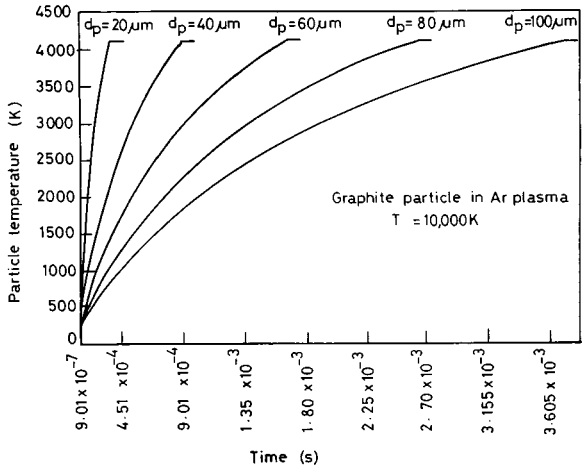

Fig. 7. Temperature history of the graphite particle for selected particle diameters.

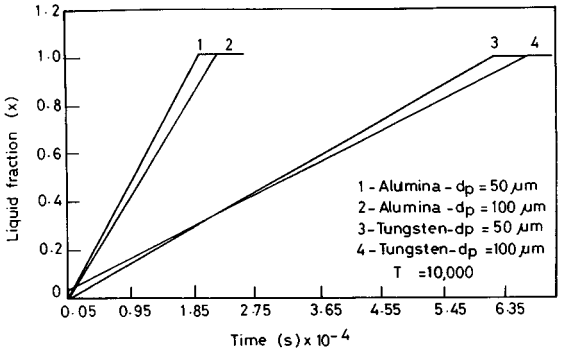

Fig. 8. Liquid fraction of the particle as a function of time for selected values of particle diameter.

Liquid fraction (x) of the alumina and tungsten particles as a function of log time for two different diameters (50 μm and 100 μm) are reported in Figure 8. For a completely molten droplet, the liquid fraction is 1, and it is evident that a particle with a larger size takes longer time to get liquefied. The liquid fraction is linear with log time

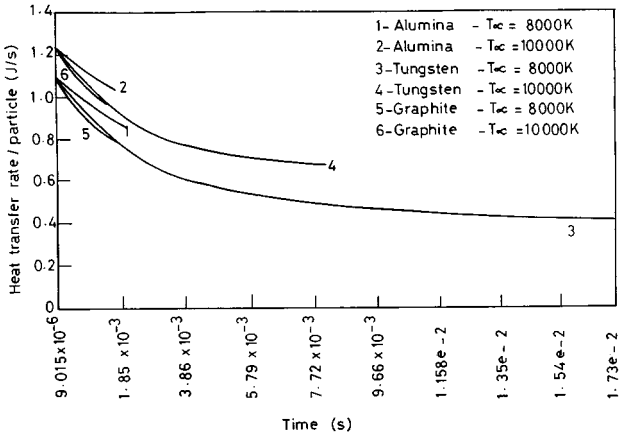

Fig. 9. Rate of heat transfer to each particle (alumina, tungsten and graphite) as a function of time for selected values of plasma temperature.

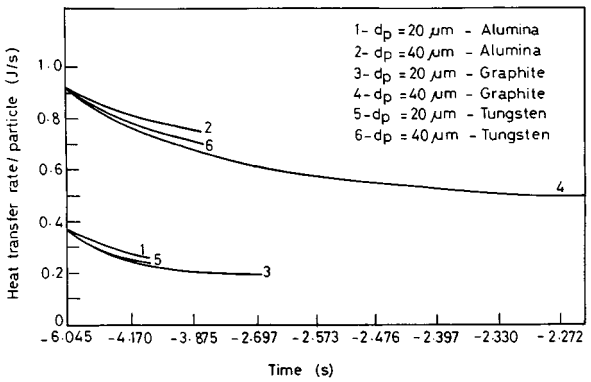

Fig. 10. Rate of heat transfer to each particle (alumina, tungsten and graphite) as a function of time for selected values of particle diameter.

indicating a relation of the type $e^x = t$ till the melting of the particle. The time for complete melting of particle $t_m = 1.98$ ms and $t_m = 5.71$ ms for alumina particle of size 50 μm and 100 μm respectively. For a given material the ratio of times t_m^{50}/t_m^{100} is 0.346 for alumina particle and for tungsten the ratio $t_m^{50}/t_m^{100} = 0.352$. For 50 μm sized (d_p) particle the time for complete melting for alumina and tungsten were 5.71 and 0. 96 ms respectively.

3.3 Heat transfer rate to the particle

Rate of heat transfer to each particle by conduction, convection and radiation as a function of log time for particles of three materials at different plasma temperatures and particle sizes are reported in Figures 9 and 10.

Heat transfer rate from plasma to the particle decreases with time for all the particles (Figs. 9 and 10). For alumina particle the heat transfer rate may be given by the relation $e^{-h_r} = ct$, where c is a constant.

For a given material, the heat transfer is higher at higher plasma temperatures. For example at $t = 10$ ms, $h_{r\,10000}/h_{r\,8000} = 1.150$, 1.159 and 1.165 for alumina, tungsten and graphite particles respectively. Also h_r is higher

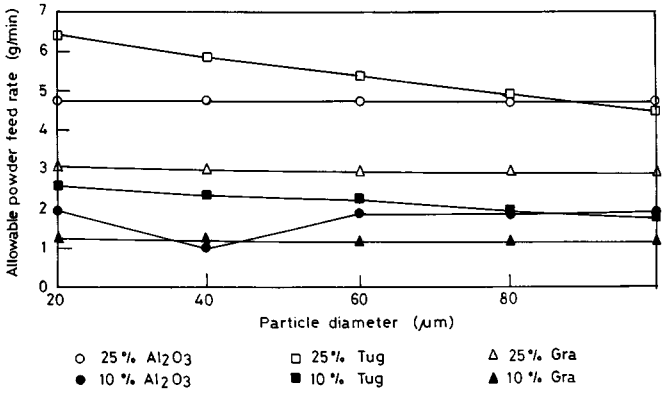

Fig. 11. Allowable powder feed rate for particle as a function of particle diameter for selected values of utilization of power in plasma.

for larger size particles; at $t = 10$ ms, $h_{r\,40\,\mu m}/h_{r\,20\,\mu m} = 3.212$, 3.270 and 3.23 for alumina, tungsten and graphite particles respectively.

From Figure 9 it is seen that, the heat transfer rate per particle (h_r), decreases with increase in time. h_r is higher for alumina particle and lower for tungsten particle. Heat transfer rate is higher at higher plasma temperatures. Heat transfer rate is depending on the temperatures of the plasma and the particle and its residence time in plasma. In our calculation T_∞ is fixed and T_p is allowed to increase up to boiling temperature of the particle. So the term $(T_\infty - T_p)$ in equation (13) is lower for tungsten particle, since it has a higher boiling temperature than those of alumina and graphite. At 10^{-2} s after the injection of the particle, h_r is 1.175, 1.051 and 1.0416 J/s for alumina, graphite and tungsten particles respectively at $T_\infty = 10\,000$ K.

Heat transfer rate as a function of log time for different particle diameters is shown in Figure 10. Heat transfer rate is higher for the particles having bigger size. It is evident that the heat transfer co-efficient is inversely proportional to the diameter of the particle. Thursfield *et al.* [27] calculated the h for different sizes of the particles. They reported that h was higher for particles with smaller in size. 10 ms after the injection of the particle into the plasma, the differences in h_r for 40 and 20 μm size particles of alumina, graphite and tungsten were 0.555, 0.519 and 0.529 J/s respectively.

3.4 Allowable powder feed rate

Allowable powder feed rates (A_p) for three powders as a function of particle diameter are shown in Figure 11. A_p values were calculated for 10 and 25% of the utilisation of the plasma power (α) ($E = 10.4$ kW, $L = 6$ mm, $D = 6$ mm and $G = 20$ l/min). A_p is seen to increase with decrease in diameter of the particle. For higher utilisation of power, A_p is higher. The value of A_p is higher for tungsten particle compared to alumina and graphite particles. This is due to the reason that, tungsten has a higher density (19 350 kg/m^3), *i.e* four times higher than

Table 1. Calculated values of Q for a 25% utilization of plasma power.

d_p	Alumina	Tungsten	Graphite
μm	Q (Cal)	Q (Cal)	Q (Cal)
20	7.330×10^{-5}	2.614×10^{-4}	6.212×10^{-4}
40	5.860×10^{-4}	2.289×10^{-3}	5.053×10^{-4}
60	1.975×10^{-3}	8.381×10^{-3}	1.726×10^{-3}
80	4.693×10^{-3}	2.165×10^{-2}	4.118×10^{-3}
100	9.173×10^{-3}	4.633×10^{-2}	8.132×10^{-3}

that of alumina (4 005 kg/m^3) and nine times greater than the graphite particle (2 195 kg/m^3). In general there is not much variation in allowable powder feed rate with increase in size of the particle except for alumina at 25% of α. Boulos *et al.* [11] calculated the A_p for alumina particle at different diameters at 10% utilisation of plasma power in rf plasma torch and the results are in agreement with the present values.

The calculated total heat transfer to the particle is seen to decrease with increase in particle size, The value of Q of the particle materials at different particle diameters is shown in Table 1. The results are in agreement with the earlier results [7,27,28].

4 Conclusions

Temperature histories of the particles in flight were studied in argon plasma. The results showed that E, G, L and D, d_p, and V_{p0} are important parameters in influencing the velocity of the particle. Careful choice of the above said parameters is important for good quality coating. By decreasing the particle size and increasing the power level and the particle residence time, we can enhance the heat transfer to the particles in plasma. The particle velocity and heat transfer from plasma to the particle are important parameters for obtaining quality coatings through plasma spraying.

The authors acknowledge the award of research project No. SP/I2/KC-16/93 by the Department of Science and Technology, Government of India and the award of Senior Research Fellowship by the Council of Scientific and Industrial Research to R.R.

Appendix

Nomenclature

a_p - area of the particle (m^2),
A_p - allowable powder feed rate (g/min),
C_{Dc} - drag co-efficient with correction factor,
C_{Df} - drag co-efficient without correction factor,
C_{pc} - specific capacity of the coolant (J/kg K),
C_p - specific heat capacity of the particle (J/kg K),
D - nozzle diameter (mm),
d_p - diameter of the particle (μm),
E - input power to the torch (kW),
G - gas flow rate of the plasma gas (l/min),
h - heat transfer co-efficient (W/m^{2}K),
h_r - rate of heat transfer to each particle (J/s),
H_{0g} - enthalpy of the incoming gas (J/kg),
H_g - enthalpy of the plasma jet (J/kg),
I - arc current (A),
$\overline{k}$ - integrated mean thermal conductivity of the plasma (W/mK),
L - nozzle length (mm),
m - mass of the particle (kg),
Nu - Nusselt number,
P - pressure (N/m^2),
Q - total heat load transferred to the particle (Cal),
Q_T - total energy to the torch (W),
Q_L - energy loss in the torch (W),
Q_G - energy in plasma gas (W),
Re - Reynolds number,
t - time (s),
t_r - total residence time (s),
T_a - ambient temperature (300 K),
T_f - film temperature (K),
T_p - particle temperature (K),
T_w - wall temperature (K),
T_∞ - plasma temperature (K),
ΔT_0 - temperature rise in coolant without arc operating (K),
ΔT_f - temperature rise in coolant with arc operating (K),
V_p - particle velocity (m/s),
V_{p0} - injection velocity (m/s),
V_g - gas velocity (m/s),
W_g - mass flow rate of the gas (kg/s).

Greek symbols

ρ - density of the plasma jet (kg/m^3) (in Eq. (7)),
$\overline{\rho}$ - integrated mean density of the plasma,
ρ_f - density of the plasma at film temperature,
ρ_p - density of the particle material,
ρ_w - density of the plasma at wall temperature,
ρ_∞ - density at the plasma temperature,
$\overline{\mu}$ - integrated mean value of the viscosity of the plasma (kg/m s),
μ_f - viscosity of the plasma at film temperature (kg/m s),
$\overline{\nu}$ - integrated mean value of the kinematic viscosity of the plasma ($\overline{\rho}/\overline{\mu}$),
ν_∞ - kinematic viscosity at plasma temperature,
λ_m - latent heat of melting of the particle (J/kg),
η - electrothermal efficiency of the torch,
ε - emissivity,
σ - Stefan's constant.

References

1. D.C. Schram, M.C.M. van de Sanden, in *Proc. IEE Colloquium on Atmospheric discharges for chemical synthesis* (IEE, London, 1998), p. 6/1-4.
2. C.F.M. Borges, M. Asmann, E. Pfender, J. Herberlin, Plasma Chem. Plasma Process. **18**, 305 (1998).
3. P.R. Taylor, M. Manrique, in *Proc. Fabrication and Advanced materials IV* (TMS, USA, 1996), p. 827.
4. C.P. Stefanovic, D. Cvetinovic, P.B. Pavlovic, Z.G. Kostic, *Proc. XXIII ICPIG* (EDP Science, France, 1997), p. 92.
5. N.N. Sayegh, W.H. Gauvin, Am. Inst. Chem. Engng. **13**, 181 (1976).
6. C. Borgianni, M. Capitelli, F. Cramrossa, L. Trilio, E. Molirance, Combust. Flame **13**, 181 (1976).
7. J.M. Houben, in *Proc. 9th Int. Thermal Spray. Conf.* (Netherlanda Inst. Voor Lastechnik, The Hague, 1980), p. 141.
8. E. Bourdin, P. Fauchais, M.J. Boulos, Int. J. Heat. Mas. Trans. **26**, 576 (1983).
9. M. Verdelle, A. Verdelle, P. Fauchais, M.I. Boulos, Am. Inst. Chem. Engng. **29**, 236 (1983).
10. N. El-Kaddah, J. Mckelliget, J. Szekely, Metall. Trans. **59**, 236 (1984).
11. M.I. Boulos, IEEE Trans. Plasma Sci. **PS-6**, 93 (1978).
12. I.G. Sayce, Pure Appl. Chem. **48**, 215 (1976).
13. E. Pfender, Pure Appl. Chem. **57**, 1179 (1985).
14. E. Pfender, Y.C. Lee, Plasma Chem. Plasma Process. **5**, 211 (1985).
15. P.D. Johnston, Combust. Flame. **189**, 373 (1972).
16. R. Ramasamy, V. Selvarajan, Comput. Mater. Sci. **15**, 265 (1999).
17. K. Ramachandran, V. Selvarajan, Comput. Mater. Sci. **6**, 81 (1996).
18. D.K. Das, R. Sivakumar, Acta Metall. Mater. **38**, 2187 (1990).
19. J.H. Park, S.H. Hong, J. Kor. Phys. Soc. **31**, 753 (1997).
20. J.M. Bauchire, J.J. Gonzalez, P. Proulx, *Proc. XXIII ICPIG* (EDP Sciences, France, 1997), p. 206.
21. P. Proulx, J.T. Mostaghimi, M.I. Boulos, Int. J. Heat Mass Trans. **28**, 1327 (1985).
22. Xi Chen, E. Pfender, Plasma Chem. Plasma Proc. **2**, 293 (1982).
23. T. Yoshida, K. Akasi, J. Appl. Phys. **48**, 2552 (1977).
24. R. Ramasamy, V. Selvarajan, K. Ramachandran, Plasma Dev. Oper. **5**, 180 (1996).
25. R. Ramasamy, V. Selvarajan, Eur. Phys. J. AP **7**, 87 (1999).
26. W.E. Ranz, W.R. Marshall, Chem. Eng. Prog. **48**, 141 (1952).
27. G. Thursfield, G.J. Davix, Trans. Instn. Chem. Engrs. **52**, 273 (1974).
28. B. Waldi, *Int. Round Table on Plasma* (Odeill, Farance, 1975).